  Bull. Chem. Soc. Jpn., 57, 2809—2815 (1984)

Electrodic Properties and Surface Characteristics of Ni-V Alloys for Water Electrolysis Cathode Materials

Ken-ichi MACHIDA, Michio ENYO,* Keisuke OGURO,† and Masanori NAKANE†
Research Institute for Catalysis, Hokkaido University, Sapporo 060
†*Government Industrial Research Institute, Midorigaoka, Ikeda-shi, Osaka 563*
(Received May 21, 1984)

Hydrogen evolution reaction on a series of hydrogen absorbing Ni-V alloys, *viz.* Ni_2V, NiV, and NiV_3, before and after pretreatments with aq HF was studied in 1 M NaOH (1 M=1 mol dm^{-3}) at 288—333 K by a galvanostatic overpotential transient technique. Results are related with the surface characteristics revealed by XPS techniques. It is concluded that the Ni in the Ni-V alloys is mainly responsible for their electrochemical properties and that the reaction proceeds *via* the Volmer-Tafel reaction route with mixed rate-determining characteristics: The activation heats are 7.7, 6.8, and 6.8 kcal mol^{-1} (1 cal=4.184 J) for two elementary steps, Volmer and Tafel, and the overall reaction, respectively. The electrocatalytic activity of the Ni-V alloys, particularly NiV_3, is drastically enhanced through the treatment with aq HF, and this is in parallel with the formation of porous Ni layers on their surface, namely the increase of the effective surface area. Potentiality of the alloys for water electrolysis cathode materials is indicated by a higher electrocatalytic activities of the Ni-V alloys over ordinary Raney nickel electrodes. Hydrogen absorbability of the alloys was also investigated: NiV_3 stored hydrogen up to [H]/[M]=$\leq$0.3 after a cathodic polarization at about −400 mV hydrogen overpotential, but that in Ni_2V or NiV was far smaller.

Overpotential is one of the major factors which decrease efficiency of electrochemical processes and, accordingly, the electrode is often made to possess a large surface area.[1] We have reported recently that a series of amorphous Ni-Ti and Ni-Zr alloys after a brief treatment with aq HF attain a high electrocatalytic activity for the hydrogen electrode reaction (HER). Surface characterizations including XPS observations indicated that this is due to formation of a porous layer rich in nickel on their surface during the acid treatment, similar to usual Raney nickel electrodes.[2]

The Raney nickel materials are usually prepared from Ni-Al or Ni-Zn alloys by leaching Al or Zn out with alkaline solutions. Further, we have shown in a previous paper[3] that essentially the same electrocatalytic activity is obtained by the use of aq HF as the developer instead of aq NaOH. Since V is rapidly soluble in aq HF as compared with Ni, similar to Ti or Zr, we may apply it in developing a series of Ni-V alloys.

Various elements including those of Va group such as V are known to form hydrides,[4] and thus noted as hydrogen storage materials, similar to a series of alloys containing rare earth elements.[5] The element V itself has a high hydrogen absorbability and forms nonstoichiometric hydrides up to [H]/[V]=2.0 at ambient pressure and temperature.[6] Further, effects of Ti, Cr, Fe, and Co as alloying elements on the hydrogen solubility of V-based alloys have been reported by Eguchi and Morozumi[7] or Lynch *et al.*[8]

In the Ni-V system, there are four types of intermetallic compounds (Ni_3V, Ni_2V, NiV, and NiV_3) which crystallize with tetragonal (I4/mmm),[9a] orthorhombic (Immm),[9b] tetragonal ($P4_2/mmm$),[9c] and cubic (Pm3n)[9d] systems, respectively. However, no systematic study has so far been reported on their hydrogen storage property.

The HER on many electrocatalytically active metals in aqueous solutions consists of two elementary steps, *viz.* the discharge of proton (in acidic solutions) or water (in alkaline solutions), the Volmer step, and the recombination of hydrogen adatoms H(a), the Tafel step.

Volmer step:

$$H^+B + e \rightleftarrows H(a) + B \quad (B=H_2O, OH^-), \qquad (1)$$

Tafel step:

$$2H(a) \rightleftarrows H_2. \qquad (2)$$

Use of thin foils of hydrogen permeating metals or alloys as hydrogen electrodes has a particular advantage in the mechanistic studies: The kinetics of the individual elementary steps of the HER can be obtained by analyzing transient rise and decay characteristics of the overpotential. The overpotential components shared by the constituent steps can individually be evaluated because of a large difference in the relaxation time constant between the Volmer step, which is very fast, and the Tafel step, which is extremely slow because of slow rate of variation in the activity of H(a) on the electrode surface.[10] The same technique may be applied to the Ni-V alloys to derive kinetics of the individual elementary steps and determine the mechanism of the HER.

Experimental

Preparation of Electrodes. The alloy ingots (about 5 g) with compositions of Ni_2V, NiV, and NiV_3 were synthesized from Ni (99.9%) and V (99.9%) by arc-melting as described elsewhere.[11] Their weight loss during the fabrication was negligible, or the composition of the product was essentially equal to the starting one. The alloys obtained were annealed at 1300 K for 10—15 h *in vacuo* (*ca.* 5×10^{-4} Pa), spark-cut into slices (0.5—1.0 mm in thickness), and then the surface was polished with emery papers (no. 170—200). Powder X-ray diffraction patterns of Ni_2V and NiV agreed with those in the literatures,[9b,c] but not for NiV_3 [the powder data (d_{obsd}/Å and I/I_o) observed within $(\sin\theta)/\lambda<0.50$ Å^{-1} were as follows: 2.33, 60; 2.19, 60; 2.13, 55; 2.08, 45; 2.02. 100; 1.99, 85; 1.94, 45]. The acid treatment of a series of Ni-V alloys was made with 1 M HF solution at room temperature, the period being 10 h for Ni_2V or NiV and 10—30 min for NiV_3, respectively.

Electrochemical Measurements. The electrodic properties of the Ni-V alloys were investigated in 1 M NaOH at

288—333 K according to the technique described previously.[2] The electrolytic solution was prepared from special grade NaOH (Merck Japan, Ltd.) with water obtained from a Millipore pure water system. A platinized Pt was used for a hydrogen reference electrode. Roughness factor (*RF*) of the test electrode was evaluated from double layer capacitance data assuming *a* value of 18 $\mu F\,cm^{-2}$ (true), usually observed on Hg electrode.

XPS Measurements. Surface analysis of the Ni-V alloys was performed using an ESCA apparatus (VG-III) with Al $K\alpha$ X-ray radiation. The binding energy values recorded were calibrated using the $4f_{7/2}$ signal (83.8 eV) from a gold plate which was employed as an internal standard. Surface sputtering by Ar^+ ion bombardment was carried out under the condition of 1—2 keV and 4—10 $\mu A\,cm^{-2}$. The depth D_s sputtered by the bombardment was estimated from the following equations,[12]

$$D_s = \frac{N_{Ar} \cdot Y \cdot M}{N_A \cdot \rho} \times 10^8\ \text{Å}, \quad (3)$$

$$N_{Ar} = \frac{I \cdot T}{1.6 \times 10^{-9}}, \quad (4)$$

where N_{Ar} is the Ar^+ ion flux density in ions per second, Y is the sputtering yield, M is the atomic weight, N_A is Avogadro's number, ρ is the density of the alloys, I is the ion current density in amperes and T is the duration of the bombardment in seconds. The Y value was deduced by averaging the sputtering yields for each pure component of the alloy, which were in turn evaluated by interpolation of the values determined by Kanaya *et al.*[12] at given Ar^+ ion energy values (1.0, 1.5, and 2.0 keV). An average atomic weight corresponding to the alloy composition was used for M.

Results and Discussion

Electrochemical Properties. The electrocatalytic activity of the nontreated (as-obtained) Ni_2V and NiV alloys for the HER was relatively high, so that the reversible HER potential was realized soon after introduction of the electrode into the electrochemical cell. The electrode of NiV_3, without the pretreatment which was performed later, did not give the potential because of its very low activity.

On metal and alloy electrodes which have high solubility as well as mobility of hydrogen in the bulk, a plateau region should appear on the short time (several seconds) galvanostatic overpotential rise and decay transient curves before the attainment of the steady-state polarization or equilibrium potential, respectively.[2,13] Such overpotential plateaus were indeed seen clearly on both the nontreated Ni_2V and NiV alloy electrodes. Typical rise and decay transient curves observed on the NiV alloy electrode are shown in Fig. 1. As discussed previously,[10] we can estimate two overpotential components, η_1 and η_2', for the step of discharge of water and the step of recombination of hydrogen adatoms, respectively.

Tafel plots of η_1 on the nontreated Ni_2V and NiV alloy electrodes both in the cathodic and anodic regions are shown in Fig. 2. The approximate symmetry of these curves about the abscissa and the slope (about 120 mV/decade) of the linear portions of the "Tafel lines" indicate that η_1 should represent the component overpotential for a one-electron transfer reaction, namely, the Volmer step. The symmetry factor (for the cathodic unidirectional current) is 0.5—0.6 near the reversible potential, as same as that observed earlier on $LaNi_5$ and Ni-Ti alloy electrodes.[2,13c] Likewise,

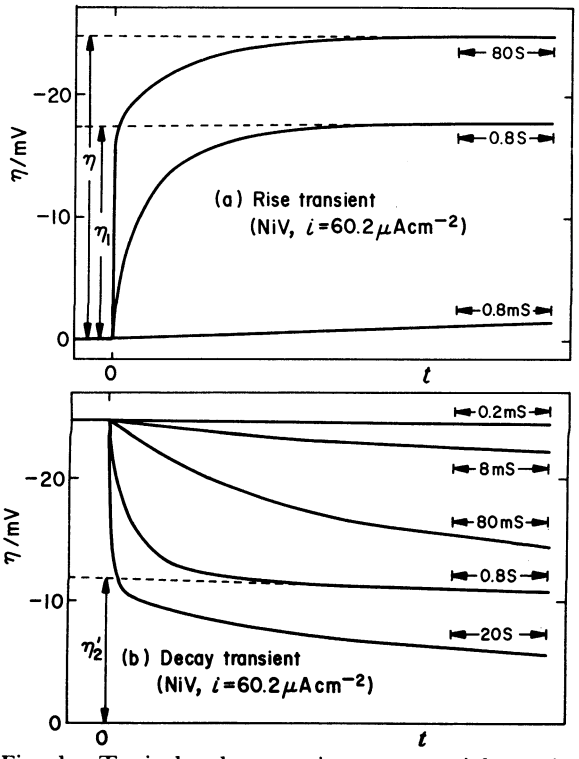

Fig. 1. Typical galvanostatic overpotential (a) rise and (b) decay transients with various time scales on a nontreated NiV alloy electrode. 1 M NaOH, 303 K. $-i$=60.2 $\mu A\,cm^{-2}$ (apparent).

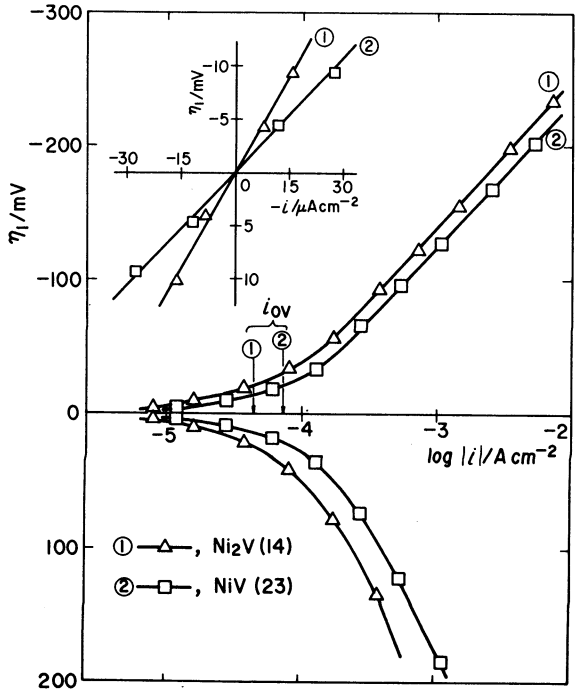

Fig. 2. Cathodic and anodic polarization behaviours of the rapidly rising overpotential component η_1 on both nontreated Ni_2V and NiV alloy electrodes. The arrows on the abscissa indicate i_{ov} as evaluated from the linear plots (the inset figure) of η_1 *vs.* i near the reversible potential. The numerals in the parentheses indicate the *RF* values. 1 M NaOH, 303 K.

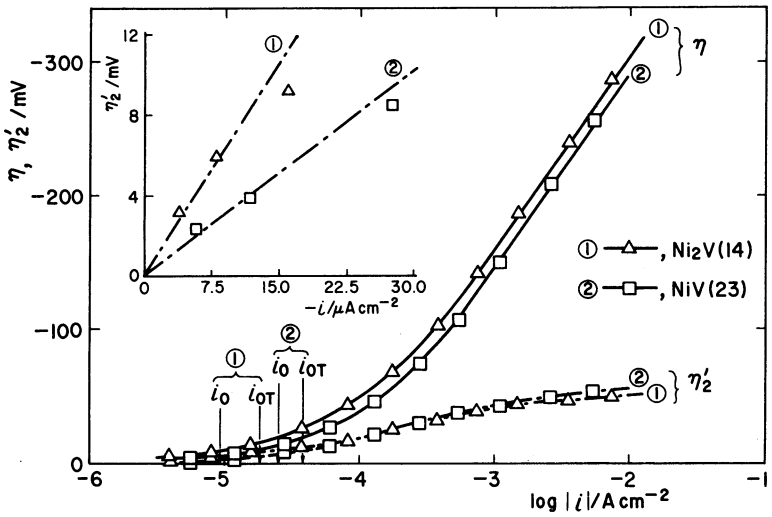

Fig. 3. Cathodic polarization behaviours of the total overpotential η and the slowly decaying overpotential component η'_2 on both nontreated Ni_2V and NiV alloy electrodes. The arrows on the abscissa indicate i_0 and i_{oT} obtained at low overpotentials (the inset figure). The numerals in the parentheses indicate the *RF* values. 1 M NaOH, 303 K.

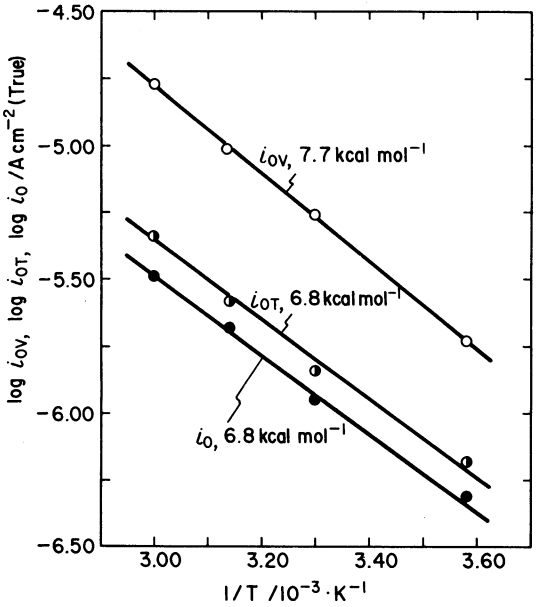

Fig. 4. Arrhenius plots of the exchange current densities for the Volmer and Tafel elementary steps and the overall reaction on the nontreated NiV alloy electrode with *RF*=29. The numerals give their corresponding activation heats. 1 M NaOH.

the approximate linearity of the cathodic η'_2 *vs.* log i behaviours with the slope of about 30 mV/decade, as shown in Fig. 3, indicates that η'_2 should be attributed to the Tafel step, as same as the case of the Pd electrode reported previolusly.[13a]

The exchange current densities of the Volmer and Tafel elementary steps, i_{oV} and i_{oT}, were obtained from the polarization resistance at low overpotentials (see the inset figures in Figs. 2 and 3) in a similar manner as the cases of other hydrogen absorbing electrodes.[13c] These values are both around the same order of magnitude, 10^{-4} A cm^{-2} (apparent) and hence, the reaction is of the mixed rate-determining type. The characteristics are similar to those of ordinary Ni electrodes. The exchange current density, i_o, of the overall reaction is readily evaluated by the relationship, $1/i_o=1/i_{oV}+1/i_{oT}$. In Figs. 2 and 3, the values of i_{oV}, i_{oT}, and i_o are respectively indicated by arrows on the abscissa.

The activation heats of the reaction steps are determined from the temperature dependences of the exchange current densities. Typical Arrhenius plots obtained on the NiV alloy electrode (*RF*=29) are shown in Fig. 4. The activation heats observed are 7.7, 6.8, and 6.8 kcal mol^{-1} for the Volmer and Tafel elementary steps and the overall reaction, respectively. These values practically agree with those determined on some Ni-based alloy electrodes, of which the reaction is also catalyzed by the nickel in the alloy matrix.[2,13c] It is noted that the heat values as well as rate data of the Tafel step and the overall reaction are close to each other. This means that the overall reaction around the reversible hydrogen electrode potential must be more intimately controlled by the Tafel step than by the Volmer step. On the other hand, the slope of the linear portion of the Tafel lines at high cathodic overpotentials is around 120 mV/decade and this is attributable to the one-electron transfer step. Necessity of variation of the overall kinetics as such in the case of the mixed rate-determining reaction has been discussed elsewhere.[10]

It is seen that the electrocatalytic activity of the specimens of the Ni-V alloys, particularly NiV_3, is drastically improved by the treatment with aq HF, along with increase in the *RF* values. Another tendency observed is that the higher the Ni content in the alloy matrix is, the higher the *RF* values attained are. Presumably, the specimen containing a larger amount of V is attacked more readily by aq HF than those of lower V content, and thus gives rise to the surface more effectively roughened.

Typical galvanostatic rise and decay behaviours on the HF-treated NiV_3 electrode are given in Fig. 5. These are similar to those of the nontreated specimens, but

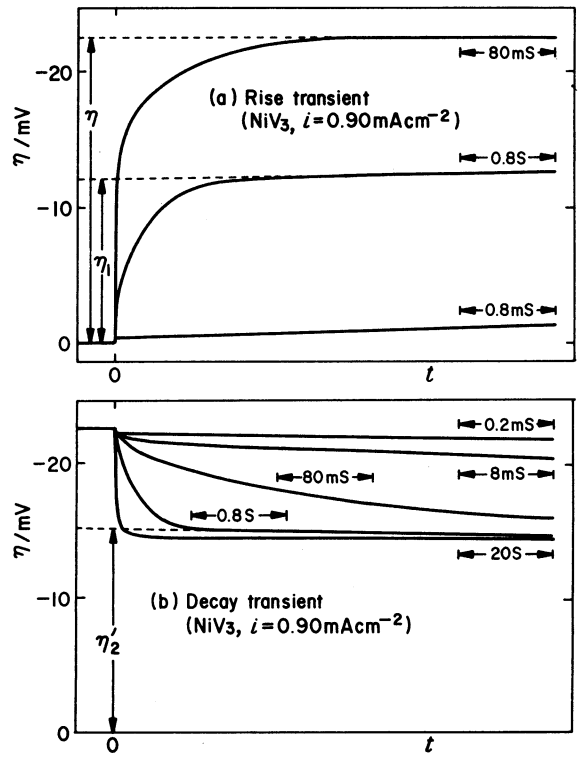

Fig. 5. Typical galvanostatic overpotential (a) rise and (b) decay transients with various time scales on a HF-treated NiV_3 alloy electrode. 1 M NaOH, 303 K. i=0.90 mA cm^{-2}.

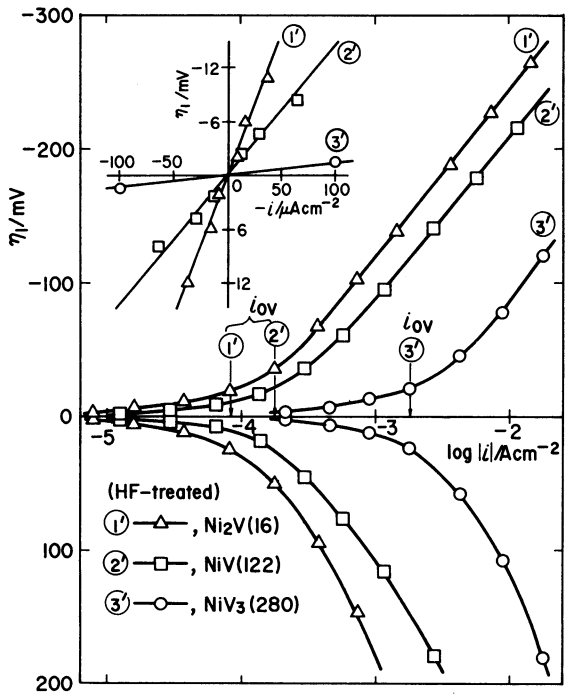

Fig. 6. Cathodic and anodic polarization behaviours of the rapidly rising overpotential component η_1 on a series of HF-treated Ni–V alloy electrodes. The arrows on the abscissa indicate i_{oV} as evaluated from the linear plots (the inset figure) of η_1 *vs.* i near the reversible potential. The numerals in the parentheses indicate the *RF* values. 1 M NaOH, 303 K.

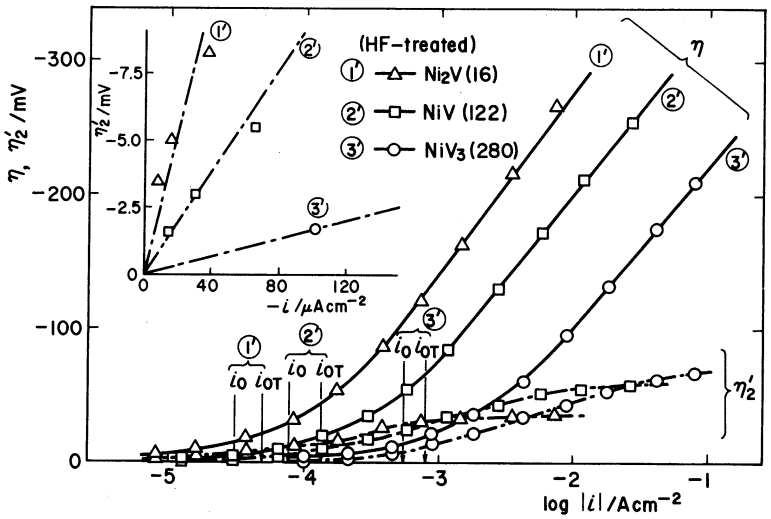

Fig. 7. Cathodic polarization behaviours of the total overpotential η and the slowly decaying overpotential component η'_2 on a series of HF-treated Ni–V alloy electrodes. The arrows on the abscissa indicate i_{oT} obtained at low overpotentials (the inset figure) and i_o evaluated by the relation of $1/i_o = 1/i_{oV} + 1/i_{oT}$. The numerals in the parentheses indicate the *RF* values. 1 M NaOH, 303 K.

the ratio η'_2/η of the HF-treated NiV_3 specimens is somewhat larger than those of the nontreated or HF-treated Ni_2V and NiV electrodes. This might indicate, on NiV_3, that the rate of diffusion in the solution phase begings to play a role in controlling the overall rate because these electrodes are highly active.

The polarization behaviours with respect to η_1, η'_2, and η on a series of HF-treated Ni–V alloys are given in Figs. 6 and 7. These characteristics are altogether essentially the same with those observed above on the nontreated electrodes.

The numerals in the parentheses in Figs. 6 and 7 represent the *RF* values of the electrodes. It is seen that the exchange current densities of the Volmer and Tafel steps, i_{oV} and i_{oT}, are almost in parallel with the *RF* values. Thus, the NiV_3 alloy electrodes which have *RF*

values of several hundreds give the i_{oV} and i_{oT} values around 10^{-3} A cm^{-2} (apparent). Yet, as the limiting current of the H_2 diffusion in solution is of the same order of magnitude with this value, the value of i_{oT} is likely to be somewhat under-estimated from the real value.

The exchange current density (i_o) of the overall reaction, evaluated by the relation $1/i_o=1/i_{oV}+1/i_{oT}$, is naturally also enhanced by the increase of the roughness. The electrocatalytic activity of the HF-treated alloys, particularly NiV_3, is as high as that of smooth of electrodes ($i_o=\leq 10^{-3}$ A cm^{-2}) on apparent surface area basis.

The HF-treated NiV_3 alloys could store hydrogen up to [H]/[M]$=\leq 0.3$ by cathodic polarization for 10—20 h at $\eta=\leq -400$ mV. (The amount absorbed in the Ni_2V and NiV specimens was negligible even after polarization for several days.) The condition with respect to hydrogen pressure P_{H_2}, to which the cathode is effectively exposed, can be obtained from the overpotential component η_2', as discussed in previous work,[14] as

$$-\eta_2' = \frac{RT}{2F} \ln P_{H_2} \qquad (5)$$

In Fig. 8, the relation between η_2' (or log P_{H_2}) and [H]/[M] ratios observed on the HF-treated NiV_3 alloy electrode (RF=530) is shown: The [H]/[M] ratios are evaluated by collecting the H_2 gas liberated from the alloy after termination of the polarization current. Also shown in this figure are typical absorption isotherms of Cr-V alloys (and not data for the Ni-V alloys, which are not available) reported by Lynch *et al.*[8] It is generally seen that the hydrogen absorbability of the V-based alloys containing Cr, Fe, or Co[7,8] is lowered with increase of the content of the added element (see Fig. 8).

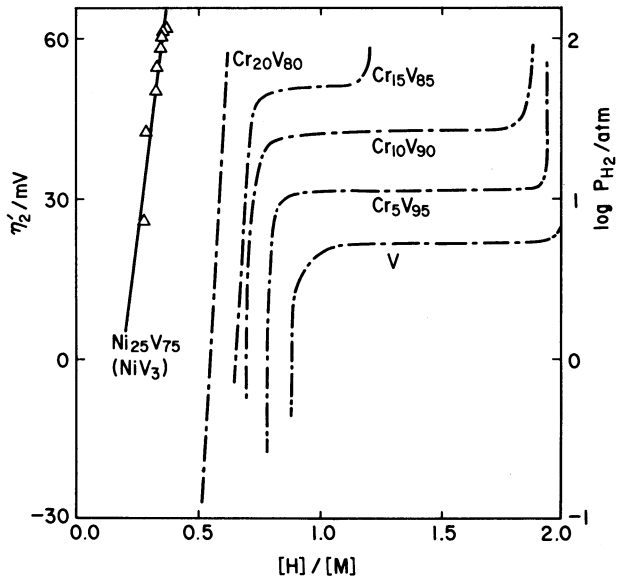

Fig. 8. Typical absorption isotherms (η_2' or log P_{H_2} *vs.* [H]/[M]) obtained on the NiV_3 alloy electrode with RF=530 after a cathodic polarization at η= 50—400 mV at 303 K for 10—20 h. The absorption isotherms of Cr-V alloys at 313 K reported by Lynch *et al.*[7] are shown for comparison.

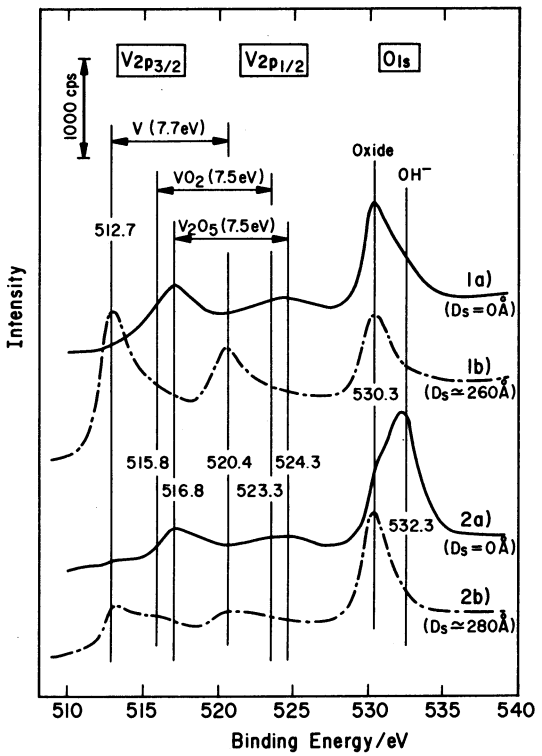

Fig. 9. XPS patterns of the V_{2p} and O_{1s} electrons on the NiV_3 alloys before (solid-lines) and after (broken-lines) Ar^+ ion bombardments up to D_s=250—300 Å, respectively. Spectra: 1a) and 1b), nontreated specimens; 2a) and 2b), HF-treated specimens.

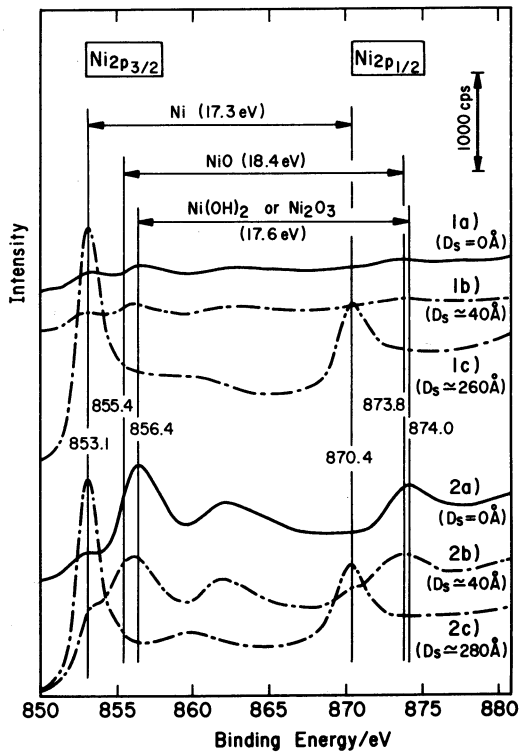

Fig. 10. XPS patterns of the Ni_{2p} electrons on the NiV_3 alloys before (solid-lines) and after (broken-lines) Ar^+ ion bombardments up to D_s=40—300 Å, respectively. Spectra: 1a), 1b), and 1c), nontreated specimens; 2a), 2b), and 2c), HF-treated specimens.

The same tendency might be expected with the Ni–V alloys, namely the larger the amount of Ni was, the smaller the amount of the stored hydrogen would be. Thus, in Fig. 8, the position of the isotherms of the NiV_3 alloy ($Ni_{25}V_{75}$) which appear at left-hand side of the line for $Cr_{20}V_{80}$ seems reasonable. The Ni–V alloys containing still smaller concentration of Ni may have a possibility as cathode materials if those of higher hydrogen absorbability are desired.

Surface Characterization. A series of XPS patterns of the Ni–V alloys have been observed before and after the treatment with aq HF. On the nontreated specimens, the signals from V are very strong compared with those from Ni. However, the spectrum intensity of Ni is drastically increased on the HF-treated Ni–V alloys, particularly NiV_3, while that of V is decreased. Typical X-ray photoelectron spectra derived from the V_{2p}, O_{1s}, and Ni_{2p} electrons on the NiV_3 alloys are given in Figs. 9 and 10, together with assignments given according to XPS data listed in a handbook.[15] (Practically the same spectra have been observed on other Ni–V alloys, *viz.* Ni_2V and NiV.)

The $V_{2p3/2}$ or $V_{2pl/2}$ signals on the nontreated and HF-treated Ni–V alloys consists mainly of two spectrum bands; The peak positions are *ca.* 515.8 and 516.8 eV for $V_{2p3/2}$ and *ca.* 523.3 and 524.3 eV for $V_{2pl/2}$, respectively. The V_{2p} spectra around 515.8 and 523.3 eV are assigned to the vanadium of VO_2 while the signals at the other peak positions are attributable to the V_{2p} electrons of V_2O_5. Signals of the metallic V become observable only after the Ar^+ ion bombardments up to the D_s of 100—200 Å. Therefore, most of the vanadium on the alloy surface exists as oxides which are probably electrocatalytically inert. This would explain the low activity of the nontreated NiV_3 alloys towards the HER.

The O_{1s} spectra on the Ni–V alloys have peaks at 530.3 and 532.3 eV, which are assigned to the oxygens of anhydrous oxides (V_2O_5, NiO, *etc*) and hydroxides (hydroxyl groups), respectively, but the latter spectrum band is significantly decreased after the Ar^+ ion bombardments ($D_s = \leq 50$ Å). This observation indicates that the hydroxides exist only near the surface.

The signals of Ni_{2p} electrons on the nonbombarded specimens appear at *ca.* 853.1, 855.4, and 856.4 eV for $Ni_{2p3/2}$ (and at *ca.* 870.4, 873.8, and 874.0 eV for $Ni_{2pl/2}$). Among them, the nickels of metal and NiO are responsible for two $Ni_{2p3/2}$ spectra (853.1 and 855.4 eV), but the remaining spectrum band is not precisely assigned to that of $Ni(OH)_2$ which is expected to exist near the surface according to the observations of the O_{1s} signal from hydroxyl groups: The same spectra have been observed on the specimens of which the hydroxyl groups are completely removed by the Ar^+ ion bombardments (see spectra 1b) and 2b) in Fig. 10). Perhaps, the Ni_{2p} spectrum bands at 856.4 and 874.0 eV may be due to the nickels of $Ni(OH)_2$ or Ni_2O_3. Signals from NiF_2 which have been observed previously on the HF-treated Ni–Al alloys[3] were not detected on a series of the HF-treated Ni–V alloys preparaed in this work.

The surface concentration ratios $C^S_{Ni/V}$ of the component metals on the nontreated and HF-treated Ni–V alloys are estimated from the integral peak intensity I of Ni_{2p} and $V_{2p3/2}$ using the following equation:

$$C^S_{Ni/V} = \frac{I_{Ni}/S_{Ni}}{I_V/S_V}, \quad (6)$$

where S is the atomic sensitivity factor for X-ray. In this work, $S_{Ni}=5.4$ and $S_V=1.4$ listed in the literature[15] are employed.

The relationships between $C^S_{Ni/V}$ and the nominal bulk compositions, $C^B_{Ni/V}$, of the Ni–V alloys before and after the acid treatments are shown in Fig. 11(a). For all the nontreated specimens, the surface Ni concentration is lower than the bulk one (below the broken-line), or the surface is enriched in V. On the other hand, the $C^S_{Ni/V}$ value of the Ni–V alloys containing a large amount of V, particular NiV_3, is significantly increased by the acid treatment. This means that the vanadium near the surface of the V-rich alloys is effectively dissolved out with aq HF and a Ni-rich layer is formed.

In Fig. 11(b), the in-depth profiles of the $C^S_{Ni/V}$ of the nontreated and HF-treated NiV_3 alloys are given. It is clearly seen that the $C^S_{Ni/V}$ value of the HF-treated specimen differs considerably from that of the nontreated one. The electrochemical capacitance data also indicate that the layer is very porous, and hence it may be considered as a kind of Raney nickel material. Consequently, the high electrocatalytic activity of the HF-treated NiV_3 alloy is concluded to be brought about by the porous Ni-rich layer formed on the surface, after leaching V out with aq HF.

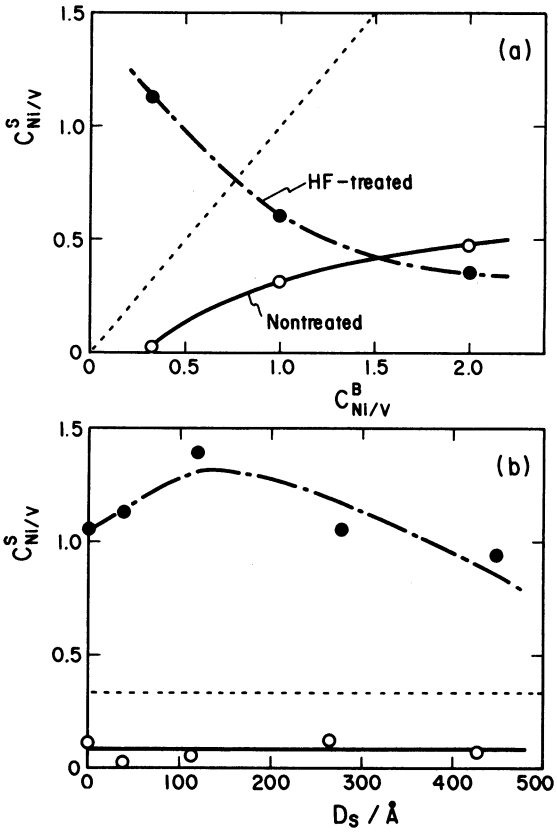

Fig. 11. (a) Relationship between the surface and bulk atomic ratios ($C^S_{Ni/V}$ and $C^B_{Ni/V}$) in a series of Ni–V alloys before and after the acid treatment. The broken line represents the case that $C^S_{Ni/V}$ equals $C^B_{Ni/V}$. (b) In-depth profiles of the surface atomic ratios $C^S_{Ni/V}$ for NiV_3 alloys before and after the acid treatment. The broken line indicates $C^S_{Ni/V}$.

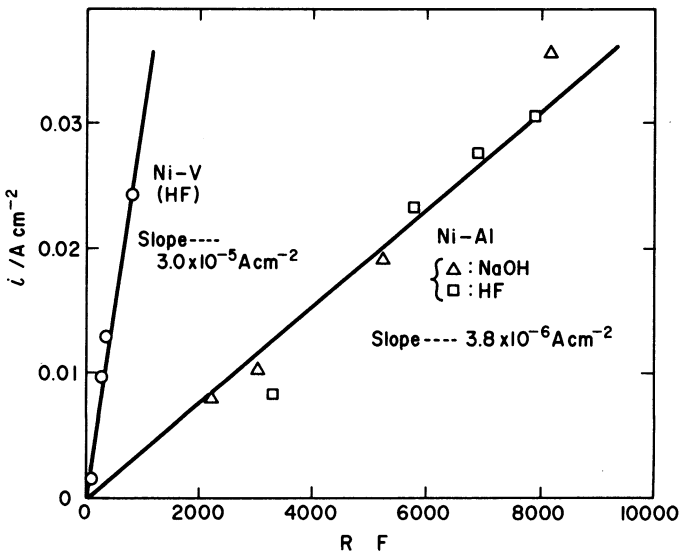

Fig. 12. Relationships between the current density (at η=−100 mV) and *RF* values on the HF-treated Ni-V alloy electrodes (○), together with those[3] on the Raney nickel electrodes treated with aq NaOH (△) and HF (□).

Synergistic Effect. It is noteworthy that a synergistic effect between Ni and V is suggested in the electrocatalytic activity on true unit surface area basis. In Fig. 12, the relation between the current density at η arbitrarily chosen at −100 mV and *RF* values on the HF-treated Ni-V alloys is shown, together with that on ordinary Raney nickel electrodes.[3] The current density on the Ni-V alloys as well as Raney nickel alloys increases linearly with the *RF* values but the slopes are clearly different. The slope (which gives the average current density per true unit surface area) is about 3.0×10^{-5} A cm^{-2} on the Ni-V alloy electrodes and this is about one order of magnitude higher than that of ordinary Raney nickel electrodes (3.8×10^{-6} A cm^{-2}). As reported elsewhere,[3] the difference in the electrocatalytic activity caused by the use of different developer, *viz.* aq NaOH or aq HF, is practically negligible. The difference in the slopes, therefore, indicates existence of a synergistic effect between Ni and V.

Conclusion

The HER on a series of the Ni-V alloy electrodes, *viz.* Ni_2V, NiV, and NiV_3, in 1 M NaOH is mainly catalyzed by nickel on the surface. The reaction proceeds *via* the Volmer-Tafel route with mixed rate-determining characteristics. The electrocatalytic activity as well as the *RF* values is drastically improved after the treatments with aq HF. On the NiV_3 alloy, in particular, the electrocatalytic activity attained is very high, being comparable with that of smooth Pt electrodes. A synergistic effect of about one order of magnitude is indicated. In view of this effect as well as their ability to produce porous Ni layers, the Ni-V alloys can be a potential candidate as a cathode material for water electrolysis.

The present work is partly supported by Grants-in-Aid for Scientific Research No. 58750629 from the Ministry of Education. Science, and Culture.

References

1) A. G. Pschenichinikov, *Int. J. Hydrogen Energy*, **7**, 51 (1982).
2) K. Machida, M. Enyo, I. Toyoshima, K. Miyahara, K. Kai, and K. Suzuki, *Bull. Chem. Soc. Jpn.*, **56**, 3393 (1983).
3) K. Machida and M. Enyo. *J. Res. Inst. Catal. Hokkaido Univ.*, in press.
4) W. M. Mueller, J. P. Blackledge, and G. G. Libowitz, "Metal Hydrides," Academic Press, New York (1968), pp. 2—7.
5) "Hydrides for Energy Storage," ed by A. F. Andresen and A. J. Maeland, Pergamon Press, New York (1978).
6) J. J. Reilly and R. H. Wiswall, *Inorg. Chem.*, **9**, 1678 (1970).
7) T. Eguchi and S. Morozumi, *Nippon Kinzokugakkai-shi*, **38**, 1025 (1974).
8) J. F. Lynch, J. J. Reilly, and F. Millot, *J. Phys. Chem. Solids.*, **39**, 883 (1978).
9) The file of X-ray powder diffraction standards by the American Society for Testing and Materials. Inorganic compounds: a), 13-523; b), 17-715; c), 7-397; d), 19-854.
10) M. Enyo, "The Comprehensive Treatise of Electrochemistry," ed by B. E. Conway *et al.* Plenum, New York (1983), Vol. 7, pp. 241-300.
11) Y. Osumi, A. Kato, H. Suzuki, M. Nakane, and Y. Miyake, *J. Less-Common Met.*, **66**, 67 (1979).
12) K. Kanaya, K. Hojou, K. Koga, and K. Toki, *Jpn. J. Appl. Phys.*, **12**, 1297 (1973).
13) a) M. Enyo and T. Maoka, *J. Electroanal. Chem.*, **108**, 277 (1980); b) M. Enyo, T. Yamazaki, K. Kai, and K. Suzuki, *Electrochim. Acta*, **28**, 1573 (1983); c) K. Machida, M. Enyo, G. Adachi, and J. Shiokawa, *Electrochim. Acta*, **29**, 807 (1984).
14) a) T. Maoka and M. Enyo, *Electrochim. Acta*, **26**, 607 (1981); b) T. Maoka and M. Enyo, *Electrochim. Acta*, **26**, 615 (1981).
15) C. D. Wagner, W. M. Riggs, L. E. Davis, J. F. Moulder, and G. E. Muilenberg, "Handbook of X-Ray Photoelectron Spectroscopy," Perkin-Elmer Co., Physical Electronics Div. (1979).